Characterization of a Lightly Loaded Underfloor Catalyzed Gasoline Particulate Filter in a Turbocharged Light Duty Truck

Stanislav V. Bohac
U.S. Environmental Protection Agency,
Ann Arbor, MI 48105
e-mail: bohac.stani@epa.gov

Scott Ludlam
U.S. Environmental Protection Agency,
Ann Arbor, MI 48105
e-mail: ludlam.scott@epa.gov

A test program to characterize the benefits and challenges of applying a European series production catalyzed gasoline particulate filter (GPF) to a U.S. Tier 2 turbocharged light duty truck (3.5 L Ecoboost Ford F150) in the underfloor location was initiated at the U.S. Environmental Protection Agency. The turbos and underfloor location keep the GPF relatively cool and minimize passive regeneration relative to other configurations. This study characterizes the relatively cool GPF in a lightly loaded state, approximately 0.1–0.4 g/L of soot loading, using four test cycles: 60 mph steady-state, 4-phase Federal Test Procedure city drive cycle (FTP), highway dirve cycle, and US06. Measurements include GPF temperature, soot loading, GPF pressure drop, brake thermal efficiency (BTE), CO_2, particulate matter (PM) mass, elemental carbon (EC), filter-collected organic carbon (OC), CO, total hydrocarbons (THC), and NO_x emissions. The lightly loaded underfloor GPF achieves an 85–99% reduction in PM mass, a 98.5–100.0% reduction in EC, and a 65–91% reduction in filter-collected OC, depending on test cycle. The smallest reductions in PM and EC occur in the US06 cycle due to mild GPF regeneration caused by GPF inlet temperature exceeding 500 °C. EC dominates filter-collected OC without a GPF, while OC dominates EC with a GPF. Composite cycle CO, THC, and NO_x emissions are reduced by the washcoat on the GPF but the low temperature location of the GPF does not make best use of the catalyzed washcoat. Cycle average pressure drop across the GPF ranged from 1.25 kPa in the four-phase FTP to 4.64 kPa in the US06 but did not affect BTE or CO_2 emissions in a measurable way in any test cycle.
[DOI: 10.1115/1.4056047]

Introduction

As of 2021, 21 million Americans live in PM2.5 (particulate matter less than 2.5 μm) nonattainment areas as defined by the 2012 PM2.5 National Ambient Air Quality Standards [1], and since most PM2.5 sampling locations collect background PM, many more Americans are exposed to elevated PM2.5 and nanoparticles because they spend time near roadways with elevated PM concentrations [2]. Light-duty gasoline vehicles are significant contributors to mobile source primary PM2.5 emissions. The Environmental Protection Agency (EPA) 2017 National Emissions Inventory reports that light-duty gasoline vehicles emitted nearly as much PM2.5 (18.4% of total mobile source PM2.5) as heavy-duty on-road diesel (21.2%) and nonroad diesel (22.3%) in 2017 [3]. 65% of light-duty gasoline vehicle PM2.5 was from exhaust while the remainder was from brake and tire wear [3]. EPA Tier 3 light-duty vehicle emissions standards (2017–2024 phase in) reduce PM certification emissions relative to Tier 2 but several technologies for further reductions exist.

One way to reduce exhaust PM from gasoline vehicles is through the application of gasoline particulate filters (GPF). GPF technology is used to achieve compliance with European Euro 6d and Chinese CN 6a solid particle number (PN) standards from pure gasoline direct injection (i.e., no port injectors) passenger cars and light commercial vehicles. In contrast, PM standards in the U.S. continue to be driven by mass emission limits rather than number, e.g., EPA Tier 3 and California Air Resources Board LEV III (low-emission vehicle), which are not sufficiently stringent to drive adoption of GPF technology. The composition of the U.S. light duty vehicle fleet also differs from its European and Chinese counterparts by its large share of chassis-certified gasoline-fueled body-on-frame trucks.

Gasoline particulate filter technology has been studied for some time [4,5] but gaps in understanding remain. Many studies address GPF installations in a close coupled position [6], or on naturally aspirated vehicles [7], each of which tends to keep the GPF at relatively high temperature. A turbocharged engine with an underfloor GPF represents the lower temperature bound for a practical GPF application on a nonhybrid vehicle. Passive regeneration is reduced, which improves filtration efficiency, but periodic active regeneration is necessary to avoid overloading the GPF.

Prior studies have often not specified the loading state of the GPF under investigation, which affects filtration and pressure drop. Previous studies have often limited GPF testing to the Federal Test Procedure city drive cycle (FTP) and aggressive drive cycle (US06), or have focused on solid PN from passenger cars since PN is the primary forcing metric in European and Chinese particulate regulations and most personal vehicles are passenger cars in those markets, unlike in the U.S. where PM mass continues to be the metric and light duty truck sales remain high.

The objective of this study is to characterize the performance of a European series production GPF in a lightly loaded state (approximately 0.1–0.4 g/L soot loading) installed in the underfloor location on a U.S turbocharged light duty truck, which keeps the GPF relatively cool and minimizes passive regeneration. Test cycles include 60 mph steady-state, FTP, highway drive cycle (HWFET), and US06. Measurements include GPF temperature, soot loading, GPF pressure drop, brake thermal efficiency (BTE), CO_2, PM mass, elemental carbon (EC), filter-collected organic carbon (OC), CO, total hydrocarbons (THC), and NO_x emissions.

Experimental Setup

The test vehicle is a 2011 Ford F150 with a 3.5 L V6 Ecoboost engine, six-speed automatic transmission, rear-wheel drive, and 17,500 miles (28,160 km). The engine uses wall-guided gasoline

Manuscript received August 28, 2022; final manuscript received September 18, 2022; published online November 29, 2022. Editor: Jerzy T. Sawicki.

Table 1 EPA Tier 3 test fuel properties

Ethanol	D5599	9.50 vol. %
Aromatics	D5769	23.48 vol. %
Benzene	D5769	0.53 vol. %
Toluene	D5769	6.10 vol. %
Ethylbenzene	D5769	0.78 vol. %
m/*p*/*o*-xylene	D5769	5.01 vol. %
1,2,4-trimethylbenzene	D5769	5.62 vol. %
1,3-diethylbenzene	D5769	1.93 vol. %
1,4-diethylbenzne + n-butylbenzene	D5769	2.89 vol. %
Naphthalene + 1-methylnaphthalene + 2-methylnaphthalene	D5769	0.47 vol. %
Olefins	D6550	7.7 wt.%
Vapor pressure	D5191	9.0 psi (62 kPa)
T10	D86	53.6 °C
T50	D86	92.5 °C
T90	D86	161.2 °C
AKI (RON+MON)/2 where RON is Research Octane Number, MON is Motor Octane Number	D2699[a], D2700[a]	88.5
Sensitivity (RON-MON)	D2699[a], D2700[a]	8.0
Lower Heating Value	D240[a]	41.886 MJ/kg
H/C ratio	D5291[a]	1.991 mol/mol
O/C ratio	D5291[a], D5599	0.0320 mol/mol
Density	D4052	0.74497 g/cm^3

[a]Measured by Paragon, Livonia, MI.

direct injection (GDI), independent intake and exhaust camshaft phasing, 10:1 compression ratio, and rated power is 272 kW at 5500 rpm. Vehicle target coefficients are 145.9 N, 0.782 N/kph, 0.0663 N/kph^2 and equivalent test weight is 2494 kg. The stock aftertreatment system, comprised of two close-coupled three-way catalysts (TWC) on each cylinder bank, is unaltered in this study. The vehicle's right and left TWC front faces are 36 cm and 38 cm downstream of their respective turbine rotors. The vehicle complies with EPA Tier 2 bin 4 standards, which includes a 10 mg/mi PM limit for the FTP test cycle.

All tests used a single batch of EPA Tier 3 gasoline test fuel and a single fill of 5W-30 Motorcraft synthetic blend engine oil. Selected fuel properties are shown in Table 1. Fuel properties were measured in-house except where noted.

The vehicle was tested in two configurations. In the GPF configuration, the vehicle was retrofit with a 2019 European series production catalyzed GPF installed after the Y-pipe in place of the resonator that is normally in that position. The front face of the GPF is 173 cm and 239 cm downstream of the right and left turbine rotors, respectively. The GPF cordierite substrate is ø5.66 in. × 4 in. (ø144 mm × 102 mm), 300 cpsi (46.5 cell/cm^2), 12 mil (0.305 mm) wall thickness. The substrate has a washcoat containing Pd and Rh for TWC-type activity. The washcoat reduces the temperature at which the GPF begins to regenerate. The GPF is mounted in a ø146 mm ID × 203 mm housing using catalyst matting. The GPF can has an 83 mm long cone on either end to connect it to 64 mm exhaust pipes. The inside volume of the GPF housing and cones is 4.1 L. GPF specifications are summarized in Table 2. The GPF and engine oil were conditioned with 600 miles (965 km) on the test vehicle before the first sampling test was conducted. The last sampling test concluded with the GPF having a total of 2000 miles (3200 km) of use, therefore, ash loading during the tests was low.

Table 2 GPF specifications

GPF source	2019 European series production
Substrate material	cordierite
Substrate size	ø5.66 in. × 4 in. (ø144 mm × 102 mm)
Cell density	300 cpsi (46.5 cell/cm^2)
Wall thickness	12 mil (0.305 mm)
Washcoat	Pd and Rh for TWC-type activity
Mounting location	Underfloor, after Y-pipe

The GPF is replaced with the stock resonator in the no GPF configuration. The inside volume of the resonator is 6.1 L. No difference in vehicle sound was noticed between GPF and resonator configurations in any of the test cycles.

A light duty truck with a turbocharged engine and an underfloor GPF was selected for this study because this configuration represents the lower temperature bound for a practical GPF application on a nonhybrid vehicle. GPF temperature is low because exhaust temperature drops across the turbines and because heat loss to the ambient occurs between the engine and GPF in the underfloor location. Low GPF temperature minimizes passive regeneration, which improves GPF filtration, and allows for control of GPF loading and GPF characterization at selected levels of soot loading.

The GPF was maintained in a lightly loaded state by running a regeneration cycle before each set of four test cycles, as described in the Test Procedures section. The GPF could have been operated more heavily loaded but a regeneration cycle was run to characterize the GPF in a lightly loaded condition. Heavily loaded GPF operation will be characterized in a future study by accumulating soot to a desired level before beginning the same four test cycles. An EPA Tier 2 vehicle (a relatively early GDI application) was chosen for this study because it produces relatively high PM mass emissions with a 10 mg/mi FTP limit. A Tier 3 vehicle (3 mg/mi FTP limit) will be addressed in a future study.

Vehicle tests were performed in light-duty chassis cell D005 at the U.S. EPA National Vehicle and Fuel Emissions Laboratory (Ann Arbor, MI). The operating points and design of the test cell, including dynamometer, air handling, constant volume sampler (CVS) dilution tunnel, and particulate and gaseous criteria pollutant measurement systems are 40 Code of Federal Regulations Part 1065 and 1066 compliant [8]. The chassis cell uses a Maha (Pinckard, AL) 1.22 m roll dynamometer, AVL (Plymouth, MI) PUMA test cell controller, CVS full flow 20.3 cm dilution tunnel with adjustable flow rate, three parallel Horiba (Ann Arbor, MI) heated particulate filter samplers (DLS, HF-47, coarse particle separator with ∼2.5 μm cut at sampling conditions), Horiba MEXA-ONE C1 bag bench and MEXA-ONE D1 continuous (modal) bench.

Gasoline particulate filter inlet gas temperature is measured 6.4 cm upstream and at the centerline of the GPF substrate with a 1.6 mm K-type thermocouple. GPF substrate centerline temperature is measured 30 mm from its front and rear faces with 0.8 mm K-type thermocouples. Pressure drop across the GPF is quantified with a differential pressure sensor that was calibrated in house to 20 kPa. Pressure drop exceeded 20 kPa for 0.8 s in one of the GPF US06 test cycles, reaching a maximum of 21.3 kPa. Since the duration and exceedance were small, results are deemed to have sufficient accuracy for this study. The vehicle was secured using its trailer hitch and cooled using a US06 fan (510 m^3/min, 47 mph) with the vehicle hood open. The test cell was maintained at 20–30 °C and 7.14 gH_2O/kg dry air. Dilution air was high-efficiency particulate absorbing (HEPA) filtered test cell air.

Filter-collected EC and OC were measured using a Sunset Laboratory (Tigard, OR) model 5L OCEC Analyzer and Autoloader using National Institute for Occupational Safety and Health method 870. 1.41 cm^2 quartz filter punches are first heated to 870 °C in helium. OC volatilizes, oxidizes to CO_2 in a MnO_2 oxidation catalyst, reduces to CH_4 in a nickel reducing methanator, and is quantified with a flame ionization detector. The punch is then cooled to 550 °C in a 10/90 mixture of O_2/He and heated to 870 °C a second time. OC that is pyrolyzed during the helium phase reduces laser transmittance of the filter punch. During the O_2/He phase, pyrolyzed carbon is oxidized and then reduced to CH_4 and quantified, while laser transmittance of the punch increases. The point where laser transmittance of the filter recovers to its initial transmittance is defined as the transition between pyrolyzed carbon and EC. Carbon that volatilizes beyond this point is categorized as EC. The sum of OC and pyrolyzed carbon is output as "reported OC" and discussed in this work as OC. The flame ionization detector is calibrated at the end of each analysis using a CH_4/He calibration mixture. OC results are not adjusted to

Table 3 CVS flow, dilution factor, and sampling filter flow rates

Test cycle	CVS flow (scfm)	Cycle-average dilution factor	PTFE and quartz filter flow (slpm)[a]
60 mph			
With GPF	350	7	80
Without GPF	350	7	40
Four-phase FTP			
With GPF	290	14	60/80 phase 1 + 2/3 + 4
Without GPF	290	14	30/40 phase 1 + 2/3 + 4
HWFET			
With GPF	290	8	80
Without GPF	290	8	40
US06			
With GPF	459	7	80
Without GPF	459	7	40

[a]Reference condition of 101,325 Pa and 293.15 K.

account for the difference between OC collected by quartz versus polytetrafluoroethylene (PTFE) filters. Note that OC and EC only include the mass of carbon. They do not include hydrogen or other elements associated with PM, nor noncarbon species associated with PM.

Particulate matter for mass measurements was collected on 47 mm PTFE filters, e.g., Measurement Technology Laboratories (MTL, Minneapolis, MN) PT47DMCAN [9]. Before and after loading with PM, filters are conditioned at 22±1 °C, 9.5±1 °C dew point for a minimum of 1 h before being weighed. Filters are weighed using an MTL A250 robotic autohandler and Mettler-Toledo (Columbus, OH) XPU2 microbalance that surrounds the filter with five 500 μCi strips of Po_{210} for neutralization of static charge. The PM measurement method used can quantify emissions at levels below 1 mg/mile [10]. PM measurements ranged from 2 to 16 mg/mile except for GPF-equipped 60 mph, FTP, and HWFET tests where they averaged 0.06 g/mi. Although this is outside the normal measurement range, population standard deviation for these tests was 0.02 g/mi, indicating that the low PM measurements had reasonable repeatability. Future work will investigate the accuracy of PM mass measurements at the sub-0.1 mg/mi level.

Organic carbon and EC sampling used 47 mm quartz fiber filters (Pall Tissuquartz 7202, Port Washington, NY). Before loading with PM, quartz filters are baked at 800 °C in air for 8+ hours. Loaded filters are sealed and stored at –20 °C until they are analyzed.

Constant volume sampler flow setting, dilution factor (based on fuel and exhaust carbon content), and sampling filter flow rate for each sampled cycle are shown in Table 3. One PTFE and one quartz filter were used for each sampled cycle. Cycle-average dilution factors were maintained between 7 and 14 and sample filter flow rates were set to 30–80 slpm (45–121 cm/s). Higher filter flow was used for GPF tests to increase sample filter loading. Filter flow was set higher for phases 3 and 4 than for phases 1 and 2 to achieve regulatory phase weighting in the four-phase FTP test.

Test Procedures

A GPF regeneration cycle was run before each set of four sampling cycles (60 mph steady-state, four-phase FTP, HWFET, US06). The GPF regeneration cycle has three parts. The first part warms up the vehicle in cruise control at 60 mph for 20 min. The second part is a 23-min sawtooth drive profile of 40 accelerations to heat the GPF and 40 decelerations to deliver oxygen to the GPF while the engine goes into deceleration fuel cut off, as verified by the upstream lambda sensor. Accelerations are from 55 to 80 mph at 2.5 mph/s. GPF inlet gas temperature exceeds 600 °C on the first full acceleration and reaches 660 °C after the first few accelerations. Decelerations are coast-downs where the driver does not apply brake or throttle. Pressure drop across the GPF and soot exotherm measurements at the outlet of the GPF indicate the GPF is regenerated after 20 accelerations, but 40 accelerations are run to ensure full regeneration. The third part operates the vehicle at 60 mph for 20 min and uses GPF pressure drop to verify it was fully regenerated.

Four test cycles were run after the GPF regeneration cycle: 60 mph steady-state, four-phase FTP, HWFET, and US06. Vehicle speed during the emissions sampling portions of these cycles is shown in Fig. 1. The sampling portion of the 60 mph steady-state test is preceded by an overnight soak at 23 °C and an unsampled 20 min in cruise control at 60 mph. The sampling portion of the 60 mph test is 20 min long and is driven with cruise control. The four-phase FTP is preceded by an overnight soak at 23 °C. The four phases of the FTP are weighted according to Eq. (1). The HWFET is run right after the four-phase FTP. The sampling portion of the HWFET test is preceded by an unsampled conditioning HWFET. The US06 is run right after the HWFET. The sampling portion of the US06 test is preceded by an unsampled conditioning US06. Vehicle preparation and test procedures for the four-phase FTP, HWFET, and US06 test cycles are described in 40 Code of Federal Regulations Part 1066 [8] and the speed traces are defined in Appendix I, Part 86 [11]

$$\mathrm{FTP}\left(\frac{g}{mi}\right) = 0.43\left[\frac{m_1(g)+m_2(g)}{d_1(mi)+d_2(mi)}\right] + 0.57\left[\frac{m_3(g)+m_4(g)}{d_3(mi)+d_4(mi)}\right] \quad (1)$$

After the US06 is completed, the GPF is regenerated and the cycles are repeated a second time. Results are shown as an average of two measurements for each cycle. Test-to-test variation is shown using error bars representing plus/minus one population standard deviation, σ. After two sets of GPF tests are complete, the GPF is replaced with the stock resonator, and the same set of tests is performed two more times to characterize the stock vehicle and compare it to the GPF configuration tests.

In addition to comparing individual cycles, GPF and stock vehicle emissions are compared using a composite cycle defined as total mass emissions divided by total distance for the sampled portions of the four test cycles. The sampled distances of the four cycles are 20.0 miles (32 km) for the 60 mph test, 14.9 miles (24 km) for the four-phase FTP, 10.3 miles (17 km) for the HWFET, and 8.0 miles (13 km) for the US06 cycle. The composite cycle is representative of most real-world vehicle operation.

Results and Discussion

Temperature and Soot Loading. After the GPF is fully regenerated using the sawtooth regeneration cycle, tailpipe emissions are sampled through four test cycles: 60 mph, four-phase FTP, HWFET, and US06. GPF inlet gas temperature is shown by the upper trace in Fig. 1 and calculated GPF soot loadings are shown by the labels above the graph.

Turbochargers and the underfloor location of the GPF cause the GPF to remain relatively cool in these test cycles. Slow soot oxidation begins in a catalyzed GPF at about 500 °C [4] and this was only exceeded in the US06 cycle. Fast soot oxidation begins at around 600 °C [12] and this was not reached in any of the four test cycles. A vehicle with this engine/GPF configuration would see little passive GPF regeneration in regular use until a "soot balance point" is reached at some relatively high degree of soot loading [13]. Without passive regeneration, soot accumulates in the GPF, improving filtration efficiency and increasing backpressure. In typical light use, the vehicle would have to initiate periodic active GPF regeneration to avoid overloading the GPF. Active GPF regeneration is outside the scope of this study but will be addressed for this vehicle/GPF configuration in the future.

Figure 1 shows GPF inlet gas temperature spends much of the FTP near or below 300 °C, which as will be shown later, negatively impacts the conversion of gaseous criteria pollutants,

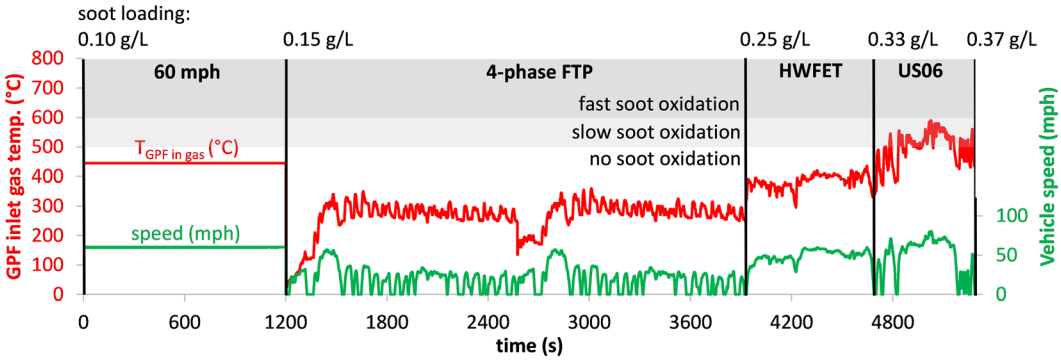

Fig. 1 GPF inlet gas temperature and soot loading

especially hydrocarbons. In a production application, the precious metal loading on the GPF would be more effective if the GPF were operated hotter (e.g., by moving the GPF closer to the engine or if the engine were naturally aspirated), or if precious metal loading on the GPF were moved to the TWC.

GPF soot loading shown at the top of Fig. 1 is calculated by subtracting measured tailpipe PM with the GPF from tailpipe PM without the GPF and normalizing by GPF volume, for the 60 mph, four-phase FTP, and HWFET cycles. Soot loading after the US06 is estimated using pressure drop across the GPF at a reference condition because the US06 causes a partial regeneration. Soot loading before the sampled portion of the 60 mph test is 0.10 g/L, which comes from the last 20 min of the sawtooth regeneration cycle and the unsampled first 20 min of the 60 mph test. Soot loading at the beginning of the four-phase FTP test is 0.15 g/L. Soot loading at the beginning of the sampled portion of the HWFET is 0.25 g/L. Soot loading at the start of the sampled portion of the US06 is 0.33 g/L. Soot loading after the sampled portion of the US06 would be 0.40 g/L if no passive regeneration occurs during the US06, but since GPF inlet temperature exceeded 500 °C, limited passive regeneration occurred. Analysis of GPF pressure drop suggests GPF soot loading is approximately 0.37 g/L after the US06.

GPF soot loading ranged from 0.10 to ~0.37 g/L (0.14–0.50 g/m^2) for the four test cycles, which is considered light loading. This puts the GPF fully in depth filtration mode assuming 0.5–2 g/m^2 wall storage capacity reported by Konstandopoulos and Papaioannou [14], or in the transition from depth to soot-cake (surface) filtration assuming 0.25 g/m^2 wall storage capacity reported by Swanson et al. [15] for a 16 mil cordierite filter.

Pressure Drop, Brake Thermal Efficiency, and CO_2. Figure 2 shows cycle-specific pressure drop across the GPF for each test cycle. The solid bars show average pressure drop across the GPF and the error bars show the range of pressure drop using a 2 s moving average window. The US06 is by far the most aggressive of the four test cycles, resulting in a cycle-average pressure drop 4.64 kPa and a maximum 2-sec pressure drop of slightly over 20 kPa. These pressure drops are higher than has been reported in several other studies [16] due to the size and characteristics of the single GPF used with a relatively high-power test vehicle. The ratio of GPF volume to to engine displacement is 0.47. Pressure drop across the resonator, which the GPF replaces, was not measured but is expected to be negligible, considering the resonator is a through-pipe with perforations opening to a larger concentric volume around the through-pipe.

The engine must perform additional work to overcome increased backpressure from the GPF. With increased backpressure the driver must use additional throttle to follow the prescribed drive trace. Increased throttle opening reduces throttling losses, which partially offset the losses from increased backpressure. Higher intake and exhaust pressures also slightly affect residual gas in the cylinder, affecting the properties of the working fluid and thermal efficiency of the engine.

A fuel-air cycle simulation was used to model the effects of backpressure, throttling losses, and working fluid properties [17,18] with an engine friction simulation [19,20]. Simulation results show that at steady engine operation ranging from 2.7 to 6.1 bar indicated mean effective pressure representing average engine loads spanning the four test cycles, about half of the pumping work needed to drive exhaust through the GPF is offset by reduced throttling and changes in working fluid properties.

Brake thermal efficiency, defined here as work performed at the chassis rolls per unit lower heating value of fuel energy, was measured with and without the GPF for each test cycle and ranged from 32.1% for the 60 mph case to 19.0% for the four-phase FTP. BTE with the GPF was indistinguishable from BTE without the GPF in every test cycle (95% confidence interval, Student's t distribution) with good test repeatability with average BTE coefficient of variation of 0.34%.

CO_2 emissions per mile ranged from 482 g/mi in the US06 to 281 g/mi in the HWFET. CO_2/mi with and without the GPF was also statistically indistinguishable for each test cycle (95% confidence interval, student's t distribution). Measurements showed good repeatability with average CO_2/mi coefficient of variation of 0.48%. Other studies have also found no measurable change in CO_2 emissions from GDI vehicles with catalyzed GPF in New European Drive Cycle, Worldwide harmonized Light vehicles Test Cycles, FTP, or US06 test cycles [7,21].

Particulate Matter, Elemental Carbon, and Organic Carbon

Figure 3 shows the GPF is very effective at reducing PM mass across all test cycles despite relatively low GPF soot and ash loading. Test repeatability is shown by error bars denoting plus/minus one population standard deviation, $\pm\sigma$. The GPF reduces PM by

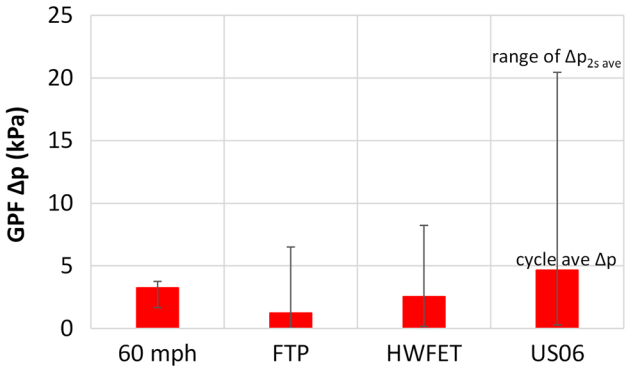

Fig. 2 Pressure drop across GPF

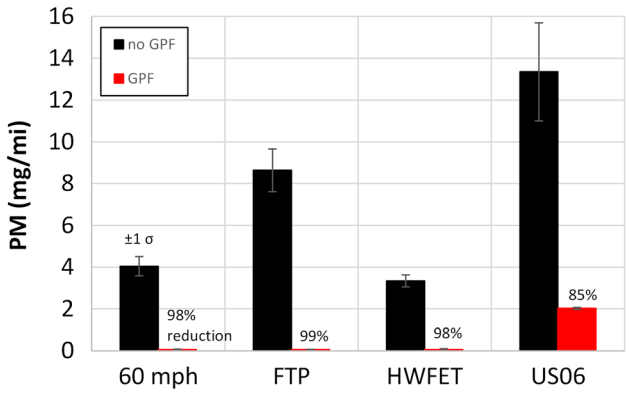

Fig. 3 PM emissions

98–99% in the 60 mph, FTP, and HWFET test cycles. PM from the GPF-equipped vehicle over these cycles was similar, ranging from 0.060 mg/mi in the 4-phase FTP to 0.062 mg/mi in the 60 mph test. Average population standard deviation was ±0.023 mg/mi. The smallest percentage decrease in PM occurs in the US06, which is likely due to mild GPF regeneration caused by the GPF inlet gas temperature exceeding 500 °C. Araji and Stokes [6] measured PM filtration in FTP and US06 test cycles and saw lower filtration efficiency, likely due to their GPF being mounted in a close-coupled (hotter) location. Chan et al. [7] also measured lower PM filtration efficiency in the FTP and especially in the US06 in a naturally aspirated (hotter GPF) test vehicle.

PM emissions without a GPF are highest in the FTP and US06 cycles. Second-by-second measurements using a TSI 3090 engine exhaust particle sizer spectrometer indicate the FTP has elevated PM emissions during cold start and the US06 has elevated emissions during fuel-rich operation.

The photographs in Fig. 4 show PTFE sample filters for 60 mph, FTP, and HWFET drive cycles are indistinguishable from new sample filters, while the no GPF sample filters are jet black. The photos visualize the 98–99% reduction in gravimetric PM shown in Fig. 3. The CVS dilution factor is the same for GPF and no GPF sample filters and the filter flow for GPF sample filters is double the filter flow for no GPF sample filters.

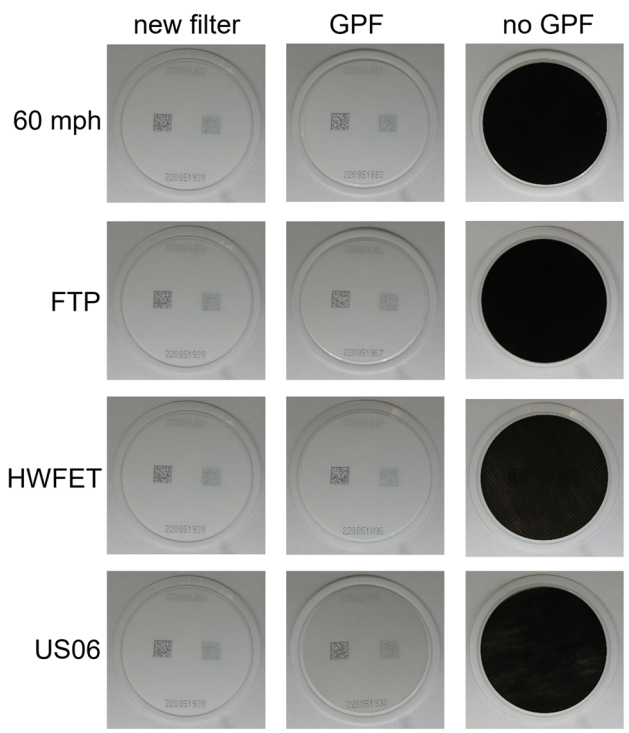

Fig. 4 PTFE sample filters

The only GPF test that generates a sample filter with a faint gray color is the US06, in agreement with the lower gravimetric PM reduction of 85% shown in Fig. 3 and the mild regeneration during this cycle. The gray color of this filter suggests a small amount of soot, not just semivolatile hydrocarbons, is emitted during regeneration.

Figure 5 shows that GPF is even more effective in reducing EC than PM. EC is reduced by 100.0% in the 60 mph, FTP, and HWFET test cycles and by 98.5% in the US06 cycle. The US06 cycle likely has the smallest percentage decrease in EC because of mild regeneration during this cycle. The small amount of GPF-out EC in the US06 cycle supports the observation of a faint gray color seen on the US06 GPF sampling filter shown in Fig. 4.

Although EC emissions quantified in this study and airborne black carbon (BC) studied by climate scientists have different operationally defined definitions, they are closely related and often used as surrogates [22]. Reduced BC emissions are beneficial for combating climate change [22]. BC has higher potency than CO_2 but a much shorter lifetime. Over a time-horizon of 100 years, the global warming potential (GWP) of BC is 910 time greater, gram for gram, than CO_2 [22]. Selecting a longer time horizon results in a smaller GWP for BC.

The lightly loaded GPF reduces EC by 6.3 mg/mi in the US06 cycle, which equates to a 5.7 g/mi reduction in CO_2, assuming the GPF does not increase fuel consumption and applying a 100-year GWP of 910. The GPF reduces EC by 4.3 mg/mi in the FTP cycle, which equates to a 3.9 g/mi reduction in CO_2.

Figure 6 shows that GPF is effective in reducing filter-collected organic carbon (OC) for all test cycles, although less than PM and EC. OC reduction ranges from 65 to 91%. The error bars in Fig. 6, denoting $\pm\sigma$, show that OC measurements have more test to test variation than PM and EC measurements.

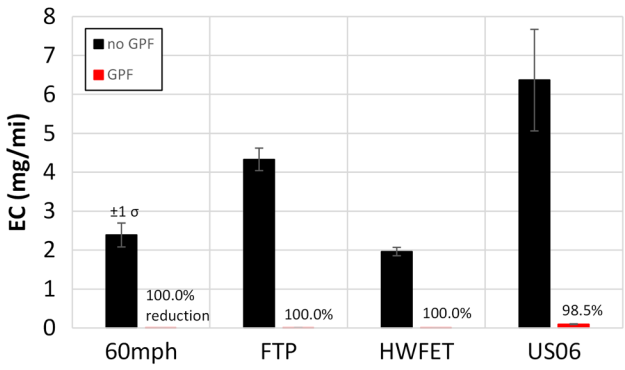

Fig. 5 Elemental carbon emissions

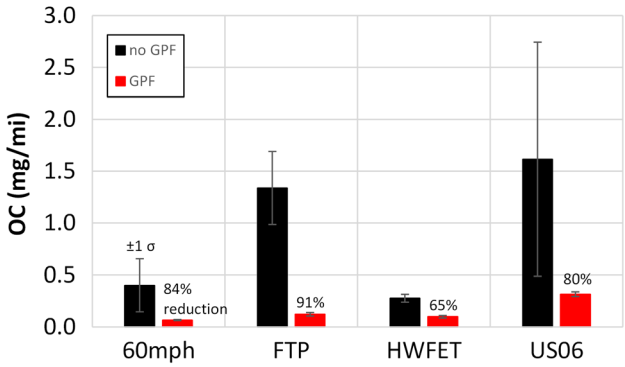

Fig. 6 Filter-collected organic carbon emissions

The sum of EC and OC is total carbon (TC). The ratio of TC (mass of carbon) to gravimetric PM (mass of everything on a PTFE filter) ranges from 60-69% for the no GPF test cycles and shows more variation for GPF test cycles where EC and OC are very low. TC is less than gravimetric PM because it does not include water, hydrogen, oxygen, nitrogen, sulfur, or ash associated with PM collected by PTFE filters.

Elemental carbon/TC ranges from 76 to 88% for the no GPF test cycles, indicating that most of the carbon in no GPF PM is in elemental form. EC/TC ranges from 0.3 to 24% for the GPF test cycles, indicating that most of the carbon in GPF PM is in the form of semivolatile hydrocarbons. The GPF is especially good at reducing EC.

Composite Cycle Emissions. The next two graphs present composite cycle emissions, defined as total mass emissions divided by total distance of the four test cycles. Figure 7 shows composite cycle PM, EC, and OC emissions without and with the GPF. The lightly loaded GPF reduces composite cycle PM, EC, and OC by 95%, 99.6%, and 85%, respectively, reflecting results from individual test cycles described earlier.

The lightly loaded GPF reduces composite cycle EC by 3.4 mg/mi, which equates to a 3.1 g/mi reduction in CO_2, assuming the GPF does not increase fuel consumption and applying a 100-year GWP of 910 from Ref. [22].

Composite cycle EC/TC is 81% for the no GPF case and 11% for the GPF case, indicating that EC dominates OC in the no GPF case, while OC dominates EC in the GPF case. The lightly loaded GPF is more effective in reducing EC than OC. This agrees with the measurements reported by Parks et al. [23].

Semivolatile organic carbon (SVOC) species are believed to be predominantly in the gaseous phase as they pass through the GPF during the majority of the test cycles because GPF inlet gas temperature is mostly between 300-600 °C as seen in Fig. 1. Some of these species are oxidized by the catalyzed washcoat on the GPF and some pass through the GPF wall without being oxidized. Since the GPF filters out most of the EC (99.6% for the composite cycle), there is much less soot for SVOC to adsorb onto post-GPF. The 85% reduction in filter-collected OC is likely partially due to the GPF washcoat oxidizing some SVOC, and partially due to there being less EC for SVOC to adsorb onto.

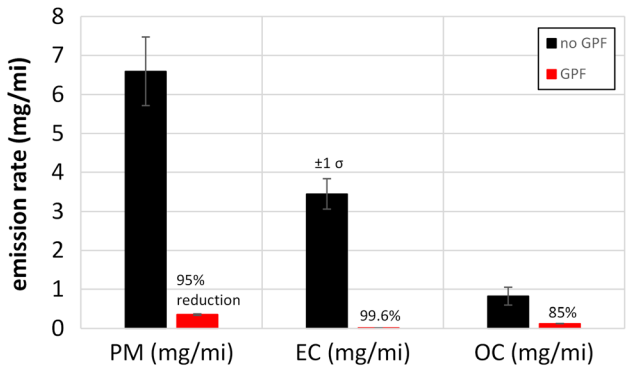

Fig. 7 PM, EC, OC emissions for composite cycle

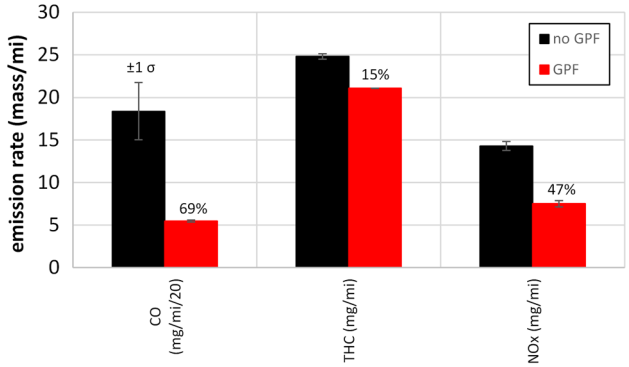

Fig. 8 CO, THC, NO_x emissions for composite cycle

Figure 8 shows composite cycle CO, THC, and NO_x emissions. The lightly loaded GPF reduces composite cycle CO, THC, and NO_x emissions by 69%, 15%, and 47%, respectively. Reductions are a result of the TWC-type activity of the washcoat on the GPF, further reducing gaseous criteria pollutants beyond what is achieved by the close-coupled TWC.

For cost reasons, it is unlikely that an underfloor GPF production implementation would retain full TWC precious metal loading and also add additional precious metal to the GPF unless a more stringent future gaseous emissions standard was targeted. Assuming current Tier 3 gaseous emissions standards, a manufacturer would more likely move precious metal from the TWC to the GPF, or not use a catalyzed washcoat on the GPF. Thus, the reductions in CO, THC, and NO_x shown in Fig. 8 may have limited relevancy in a mass production application.

The lowest relative reduction shown in Fig. 8 is for THC, at 15%. The modest reduction in THC is due to the FTP cycle, which produces the majority of composite cycle THC and maintains the GPF around 300 °C for much of the cycle, where THC conversion is hindered. Composite cycle conversions of CO and NO_x are better than THC because the emissions of these species are not dominated by the FTP cycle with its low GPF temperature.

Gasoline Particulate Filter Soot Loading and Operating Temperature. Characterization of this GPF/vehicle configuration with the GPF operating in a heavily loaded state will be addressed in a future study but results from this study and other published investigations suggest a more heavily loaded GPF, where wall pores are increasingly filled with soot and a soot cake forms on the surface, will cause higher backpressure and improved filtration efficiency for PM and filter-collected EC and OC. In this GPF/vehicle configuration, a heavily loaded GPF is likely to occur in a significant amount of real-world driving approximated by the 60 mph, FTP, and HWFET drive cycles, unless active regeneration is frequently engaged.

Naturally aspirated engines, engines without an integrated exhaust manifold, and installing the GPF close to the engine tend to increase GPF temperature. Higher GPF operating temperature will be addressed in a future study, but clearly passive regeneration will be increased and the need to engage in active regeneration will be reduced. The GPF will spend more time in a lightly loaded state and filtration efficiency will be decreased. Lighter GPF loading reduces backpressure, but higher exhaust temperature increases backpressure because the exhaust gas is less dense.

Summary and Conclusions

A light duty truck with a turbocharged engine and an underfloor GPF was chosen for this study because this configuration represents the lower temperature bound for a practical GPF application and allows for control of GPF loading. Lightly loaded GPF operation (approximately 0.1–0.4 g/L) was characterized in this study by running a regeneration cycle before each set of four test cycles. GPF inlet gas temperature remained below 500 °C during the 60 mph, four-phase FTP, and HWFET cycles and remained below 600 °C during the US06.

Cycle average pressure drop across the GPF ranged from 1.25 kPa in the four-phase FTP to 4.64 kPa in the US06 but did not affect BTE or CO_2 emissions in a measurable way in any test cycle.

The GPF reduced gravimetric PM between 85 and 99%, EC by 98.5 and 100.0% and filter-collected OC between 65 and 91%, depending on test cycle. The lowest relative reduction in PM and EC occurred in the US06 cycle due to mild GPF regeneration in that test cycle because the exhaust temperature exceeded 500 °C.

The GPF reduces EC by filtering soot from the exhaust, which is its primary function. It also reduces filter-collected OC, partially from the GPF washcoat oxidizing some SVOC, and partially from there being less tailpipe EC for SVOC to adsorb onto.

Elemental carbon/TC ratios indicate most of the sample filter-collected carbon is elemental carbon when no GPF is used (76–88% EC/TC) and most of the filter-collected carbon is organic carbon when a GPF is used (0.3–24% EC/TC).

The GPF reduced composite cycle PM, EC, OC, CO, THC, and NO_x emissions by 95%, 99.6%, 85%, 69%, 15%, and 47%, respectively. Composite cycle EC/TC is 81% for the no GPF case and 11% for the GPF case.

Disclaimer

Acknowledgment

The authors wish to thank Carl Fulper for vehicle data logging support, Luke Markham, Gurdas Sandhu, Joe McDonald, Tony Fernandez, and Ben Ellies for their helpful discussions, Michael Matthews for chassis test cell support, Michael Olechiw, Angela Cullen, and Maria Peralta for project support, and the Manufacturers of Emission Controls Association (MECA) for supplying the European series production GPF.

Nomenclature

BC = black carbon
BTE = brake thermal efficiency
CVS = constant volume sampler
EC = elemental carbon
EPA = Environmental Protection Agency
FTP = Federal Test Procedure city drive cycle
GDI = gasoline direct injection
GPF = gasoline particulate filter(s)
GWP = global warming potential
HEPA = high-efficiency particulate absorbing
HWFET = highway dirve
MON = motor octane number
MTL = Measurement Technology Laboratories
OC = organic carbon
PM = particulate matter
PM2.5 = particulate matter smaller than 2.5 μm
PN = particle number
PTFE = polytetrafluoroethylene
RON = research octane number
SVOC = semivolatile organic carbon
TC = total carbon (EC+OC)
THC = total hydrocarbons
TWC = three-way catalyst(s)

References

[1] U.S. EPA, 2021, "U.S. EPA Green Book," U.S. EPA, Washington, DC, accessed Sept. 6, 2021, https://www.epa.gov/green-book
[2] Saha, P. K., Zimmerman, N., Malings, C., Hauryliuk, A., Li, Z., Snell, L., Subramanian, R., Lipsky, E., Apte, J. S., Robinson, A. L., and Presto, A. A., 2019, "Quantifying High-Resolution Spatial Variations and Local Source Impacts of Urban Ultrafine Particle Concentrations," Sci. Total Environ., **655**, pp. 473–481.
[3] U.S. EPA, 2021, "2017 National Emissions Inventory: January 2021 Updated Release," Technical Support Document, U.S. EPA, Washington, DC, Report No. EPA-454/R-21-001.
[4] Saito, C., Nakatani, T., Miyairi, Y., Yuuki, K., Makino, M., Kurachi, H., Heuss, W., Kuki, T., Furuta, Y., Kattouah, P., and Vogt, C., 2011, "New Particulate Filter Concept to Reduce Particle Number Emissions," SAE Paper No. 2011-01-0814.
[5] Joshi, A., and Johnson, T. V., 2018, "Gasoline Particulate Filters – A Review," Emiss. Control Sci. Technol., **4**(4), pp. 219–239.
[6] Araji, F., and Stokes, J., 2019, "Evaluation of Emissions From Light Duty Trucks With and Without the Use of a Gasoline Particulate Filter," SAE Paper No. 2019-01-0971.
[7] Chan, T. W., Saffaripour, M., Liu, F., Hendren, J., Thomson, K. A., Kubsh, J., Brezny, R., and Rideout, G., 2016, "Characterization of Real-Time Particulate Emissions From a Gasoline Direct Injection Vehicle Equipped With a Catalyzed Gasoline Particulate Filter During Filter Regeneration," Emis. Control Sci. Technol., **2**(2), pp. 75–88.
[8] U.S. Office of the Federal Register, National Archives and Records Administration, 2016, "U.S. Code of Federal Regulations, Part 1066, Title 40," U.S. Office of the Federal Register, National Archives and Records Administration, Washington, DC, accessed Oct. 25, https://www.ecfr.gov/cgi-bin/text-idx?node=pt40.33.1066&rgn=div5
[9] U.S. Office of the Federal Register, National Archives and Records Administration, 2006, "U.S. Code of Federal Regulations, Appendix L, Part 50, Title 40," U.S. Office of the Federal Register, National Archives and Records Administration, Washington, DC, accessed Oct. 17, https://www.ecfr.gov/cgi-bin/text-idx?tpl=/ecfrbrowse/Title40/40cfr50_main_02.tpl
[10] Hu, S., Zhang, S., Sardar, S., Chen, S., Dzhema, I., Huang, S., Quiros, D., et al., 2014, "Evaluation of Gravimetric Method to Measure Light-Duty Vehicle Particulate Matter Emissions at Levels Below One Milligram Per Mile (1 mg/Mile)," SAE Paper No. 2014-01-1571.
[11] U.S. Office of the Federal Register, National Archives and Records Administration, 2016, "U.S. Code of Federal Regulations, Appendix I, Part 86, Title 40," U.S. Office of the Federal Register, National Archives and Records Administration, Washington, DC, accessed Oct. 25, https://www.ecfr.gov/cgi-bin/text-idx?node=pt40.21.86&rgn=div5#ap40.21.86_11931_686_11999.i
[12] Borger, T., Rose, D., Nicolin, P., Coulet, B., and Bachurina, A., 2018, "Severe Soot Oxidations in Gasoline Particulate Filter Applications," SAE Paper No. 2018-01-1699.
[13] Nicolin, P., Rose, D., Kunath, F., and Boger, T., 2015, "Modeling of the Soot Oxidation in Gasoline Particulate Filters," SAE Int. J. Engines, **8**(3), pp. 1253–1260.
[14] Konstandopoulos, A. G., and Papaioannou, E., 2008, "Update on the Science and Technology of Diesel Particulate Filters," KONA Power Part. J., **26**(0), pp. 36–65.
[15] Swanson, J., Watts, W., Kittelson, D., Newman, R., and Ziebarth, R., 2013, "Filtration Efficiency and Pressure Drop of Miniature Diesel Particulate Filters," Aerosol Sci. Technol., **47**(4), pp. 452–461.
[16] Chan, W., Meloche, E., Kubsh, J., and Brezny, R., 2014, "Black Carbon Emissions in Gasoline Exhaust and a Reduction Alternative With a Gasoline Particulate Filter," Environ. Sci. Technol., **48**(10), pp. 6027–6034.
[17] Heywood, J. B., 1988, *Internal Combustion Engine Fundamentals*, McGraw-Hill, New York.
[18] Olikara, C., and Borman, G., 1975, "A Computer Program for Calculating Properties of Equilibrium Combustion Products With Some Applications to I.C. Engines," SAE Paper No. 750468.
[19] Patton, K., Nitschke, R., and Heywood, J., 1989, "Development and Evaluation of a Friction Model for Spark-Ignition Engines," SAE Paper No. 890836.
[20] Bohac, S. V., Baker, D. M., and Assanis, D. N., 1996, "A Global Model for Steady State and Transient S.I. Engine Heat Transfer Studies," SAE Paper No. 960073.
[21] Ito, Y., Shimoda, T., Aoki, T., Yuuki, K., Sakamoto, H., Kato, K., Their, D., Kattouah, P., Ohara, E., and Vogt, C., 2015, "Next Generation of Ceramic Wall Flow Gasoline Particulate Filter with Integrated Three Way Catalyst," SAE Paper No. 2015-01-1073.
[22] Bond, T. C., Doherty, S. J., Fahey, D. W., Forster, P. M., Bernsten, T., DeAngelo, B. J., Flanner, M. G., et al., 2013, "Bounding the Role of Black Carbon in the Climate System: A Scientific Assessment," J. Geophys. Res. Atmos., **118**, pp. 5380–5552.
[23] Parks, J. E., Storey, J. M. E., Prikhodko, V. Y., Debusk, M. M., and Lewis, S. A., 2016, "Filter-Based Control of Particulate Matter From a Lean Gasoline Direct Injection Engine," SAE Paper No. 2016-01-0937.